Application of UV absorbance and fluorescence indicators to assess the formation of biodegradable dissolved organic carbon and bromate during ozonation

Application of UV absorbance and fluorescence indicators to assess the formation of biodegradable dissolved organic carbon and bromate during ozonation

Wen-Tao Li [a, b, *], Meng-Jie Cao [b], Tessora Young [b], Barbara Ruffino [c], Michael Dodd [b], Ai-Min Li [a,*], Gregory Korshin [b]

[a] State Key Laboratory of Pollution Control and Resources Reuse, School of the Environment, Nanjing University, Nanjing, 210023, China

[b] Department of Civil & Environmental Engineering, University of Washington, Box 352700, Seattle, WA 98195-2700, United States

[c] Department of Environment, Land and Infrastructure Engineering, Politecnico di Torino, Corso Duca degli Abruzzi, 24 10129 Torino, Italy

CORRESPONDING AUTHOR FOOTNOTE：

Prof. Ai-Min Li
Email: liaimin@nju.edu.cn

Wen-Tao Li
Email: liwentaoepa@hotmail.com; liwentaonju@163.com

Abstract:

This study examined the significance of changes of UV absorbance and fluorescence of dissolved organic matter (DOM) as surrogate indicators for assessing the formation of bromate and biodegradable dissolved organic carbon (BDOC) during the ozonation of surface water and wastewater effluent. Spectroscopic monitoring was carried out using benchtop UV/Vis and fluorescence spectrophotometers and a newly developed miniature LED UV/fluorescence sensor capable of rapidly measuring UVA280 and protein-like and humic-like fluorescence. With the increase of O_3/DOC mass ratio, the plots of BDOC formation were characterized of initial lag, transition slope and final plateau. With the decrease of UV absorbance and fluorescence, BDOC concentrations initially increased slowly and then rose more noticeably. Inflection points in plots of BDOC versus changes of spectroscopic indicators were close to 35-45% loss of UVA254 or UVA280 and 75-85% loss of humic-like fluorescence. According to the data from size exclusion chromatography (SEC) with organic carbon detection and 2D synchronous correlation analyses, DOM fractions assigned to operationally defined large biopolymers (apparent molecular weight, AMW>20 kDa) and medium AMW humic substances (AMW 5.5-20 kDa) were transformed into medium-size building blocks (AMW 3-5.5 kDa) and other smaller AMW species (AMW<3 kDa) associated with BDOC at increasing O_3/DOC ratios. Appreciable bromate formation was observed only after the values of UVA254, UVA280 and humic-like fluorescence in O_3-treated samples were decreased by 45-55%, 50-60% and 86-92% relative to their respective initial levels. No significant differences in plots of

bromate concentrations versus decreases of humic-like fluorescence were observed for surface water and wastewater effluent samples. This was in contrast with the plots of bromate concentration versus UVA254 and UVA280 which exhibited sensitivity to varying initial bromide concentrations in the investigated water matrixes. These results suggest that measurements of humic-like fluorescence can provide a useful supplement to UVA indices for characterization of ozonation processes.

Keywords: ozonation; biodegradable dissolved organic carbon; bromate; spectroscopic indicator; humic substances; online fluorescence sensor

1. Introduction

Ozonation has been widely used in drinking water and wastewater treatment for disinfection and oxidation purposes (Reungoat et al. 2012, von Gunten 2003a, b, Zimmermann et al. 2011). Extensive studies have shown that ozonation results in significant elimination of adverse biological effects of many organic micropollutants (e.g., endocrine disrupting chemicals, antibiotics, and pharmaceuticals) as well as removal of color, odor and taste (Dodd et al. 2009, Hollender et al. 2009, Huber et al. 2005, Lee et al. 2012, Liu et al. 2012a, Nakada et al. 2007, Peter and von Gunten 2007).

Ozone exposures required for disinfection and oxidation may result in the formation of undesirable organic and inorganic byproducts, including various disinfection byproducts (DBPs) and biodegradable dissolved organic carbon (BDOC) (von Gunten 2003b, Wert et al. 2007). Ozonation has been shown to convert relatively refractory components of dissolved organic matter (DOM) into BDOC (e.g., aldehydes, carboxylic acids, ketones and etc.) without a significant decrease in overall dissolved organic carbon (DOC) concentration (Liu et al. 2015, Nishijima et al. 2003, Wert et al. 2007). The ozonation-derived BDOC in turn largely defines the biological stability of ozonated water, as it can contribute to increases in bacterial regrowth in drinking water distribution systems or wastewater effluent receiving waters (Escobar and Randall 2001). As a result, ozonation is usually combined with a subsequent process of biological filtration to consume BDOC before the treated water is conveyed into a distribution system or a receiving water body. In this context, characterization of changes of molecular weights (MW) of DOM and evaluation of BDOC formation may

provide a better understanding of integrated O_3 biofiltration processes for DOC removal.

In addition, ozonation of bromide-containing water or wastewater leads to the formation of bromate (von Gunten and Oliveras 1998). Bromate is classified as a probable or likely human carcinogen, and many countries have established the maximum allowable level of bromate in drinking water at 10 μg/L (Butler et al. 2005). Unlike many organic DBPs, bromate is relatively stable and is difficult to remove using conventional treatment technologies (Butler et al. 2005, Nie et al. 2014). Although ecological impacts of bromate formation during wastewater ozonation are uncertain, the potential public health implications of bromate formation in potable water reuse scenarios utilizing ozonation could be significant. Hence it is of substantial interest to develop tools for better predicting and controlling bromate concentrations formed during both drinking water and wastewater ozonation.

The formation of BDOC and bromate, as well as the elimination of micropollutants, are directly related to the ozone exposure ($\int_0^t [O_3] dt$); that is, the time-dependent ozone concentration integrated over exposure time. An optimization of the ozone exposure is necessary to maximize the effect of oxidation and minimize the formation of undesired DBPs, especially BrO_3^-. However, for wastewater effluents, it is difficult to measure a dissolved O_3 residual during the initial O_3 demand stage (Gerrity et al. 2012, Wert et al. 2009). Additionally, direct analyses of BDOC and bromate are time-consuming and expensive. Therefore, the development of surrogate parameters for frequent online monitoring to enable more automated controls of ozone dosage is warranted. For example, the California Department of Public Health recently published a revised set

of draft regulations for groundwater replenishment, which requires full advanced treatment facilities to identify at least one surrogate parameter that can be monitored continuously (Chon et al. 2015, Gerrity et al. 2012).

A number of studies have examined the performance of spectroscopic indicators, such as color, differential UV absorbance (UVA) and/or total fluorescence, and shown that such indicators were correlated with the removal efficiencies of organic micropollutants during ozonation (Gerrity et al. 2012, Li et al. 2016b, Liu et al. 2012b, Nanaboina and Korshin 2010, Wert et al. 2009). Recently, Chon et al. (2015) applied the concept of electron donating capacity of DOM combined with UVA254 measurements to evaluate the degradation of micropollutants and the formation of bromate. Other studies have assessed the use of UVA254 and related indices to quantify the formation of individual ozonation byproducts associated with BDOC (Liu et al. 2012a).

Measurements of UV absorbance at 280 nm by means of UV light emitting diodes (LEDs) provide an attractive, energy-efficient alternative to conventional UVA254 monitoring (Bridgeman et al. 2015, Tedetti et al. 2013). UVA280 has previously been found to correlate well with DOM molecular weight and aromaticity and exhibit lower spectral overlap than UVA254 with inorganic species such as NO_3^- and NO_2^- that may interfere with measurements in many waters (Chin et al. 1994). In addition, measurements of DOM fluorescence at selected excitation and emission wavelengths provide a useful complement to UVA280 since fluorescence detection can also be implemented using LEDs and can enable more selective monitoring of chemically

97 reactive protein-like and humic-like DOM components (Fimmen et al. 2007, Henderson
98 et al. 2009). We recently demonstrated the use of a miniaturized LED UV/fluorescence
99 sensor – capable of online measurement of UVA280, as well as protein-like and humic-
100 like fluorescence – to predict DBP formation during chlorination (Li et al. 2016a).

101 The present study employs a sensor of this type to determine whether UVA280 and
102 fluorescence indices may be used to develop correlations with BDOC and bromate
103 formed during the ozonation of surface water and wastewater. To this end, degradation
104 of DOM chromophores and fluorophores, MW changes, and formation of BDOC and
105 bromate were examined during ozonation of a set of surface water and wastewater
106 matrixes with varying initial bromide concentrations.

107 ## 2. Material and methods

108 ### 2.1. Water matrixes and reagents

109 Three water matrixes were used in the experiments described below. Secondary
110 municipal wastewater effluent samples were taken from the West Point Treatment Plant
111 in King County, WA (WWTP-I on Dec 14th, 2015 and WWTP-II on Feb 28th, 2016).
112 This plant uses high-rate oxygen activated sludge technology without denitrification.
113 The surface water was sampled from Lake Pleasant, which is a brown water eutrophic
114 lake in Bothell, WA. Basic water characteristics of these waters are shown in **Table 1**.
115 All the water samples were immediately filtered through a 0.45 μm membrane upon
116 collection and stored at 4 ^{o}C before use.

117 The following chemicals were used in this study: sodium bromide (Sigma-

Aldrich, >99%), sodium bromate (Sigma-Aldrich, >99%), polyethylene glycol standards (Alfa Aesar), methylamine solution (Sigma-Aldrich, 40 wt. % in H_2O), and potassium indigotrisulfonate (Sigma-Aldrich).

2.2. Ozonation batch experiments

Five semi-batch ozonation experiments were performed at room temperature (25 ±2 ºC) with the three water matrixes mentioned above to explore the formation of BDOC and bromate and evolution of spectroscopic indices during exposure to ozone. For the WWTP-I water matrix (DOC 5.82 mg/L), three semi-batch experiments were undertaken with spiked bromide concentrations of 50 μg/L (WWTP-A, 322.9 μg/L total Br^-), 100 μg/L (WWTP-B, 373.8 μg/L total Br^-) and 200 μg/L Br^- (WWTP-C, 491.6 μg/L total Br^-) respectively, to explore effects of initial Br^- concentration. For the WWTP-II water matrix (DOC 6.93 mg/L), one ozonation semi-batch experiment was performed using a 100 μg/L Br^- spike (WWTP-D, 301.5 μg/L total Br^-) as a comparison with the WWTP-I experiments. Because Lake Pleasant water had a high DOC concentration (14.87 mg/L), the water was diluted 2.5 times with Milli-Q water and spiked with 100 μg/L Br^- (LP, 5.98 mg/L DOC and 116.1 μg/L total Br^-).

Ozone was generated by an oxygen-fed ozonator (IN USA AC-2025; Norwood, MA, USA). The feed gas stream containing ozone was bubbled through 200 mL WWTP effluent or 250 mL LP water samples contained in a 500 mL borosilicate glass gas-washing bottle using a sintered glass gas diffuser at a flow rate of ~550 ml/min. In each batch experiment, the ozone doses were varied as a function of ozonation times which

were 0, 2, 5, 10, 15, 20, 25*, 30, 40, 50*, 60, 100, 180 and 300** s (* specific for LP series and ** specific for WWTP series). The residual O_3 concentrations in ozonated samples were immediately measured according to the standard indigo method (Bader and Hoigné 1981), where 1 mL of ozonated sample was immediately spiked into glass vials containing 9 mL indigo solution, and then analyzed for residual absorbance at 600 nm by UV-Vis spectroscopy. The remainder of the ozonated sample volumes was transferred into 250 mL glass bottles with caps. UVA and fluorescence indicators were measured at least 2 hours after ozonation, allowing the residual ozone to naturally decay without adding any quenching agent. Then the samples were stored at 4 ^{o}C before other analyses, which were done within 5 days for each batch.

Compared with directly spiking aliquots of ozone stock (Chon et al. 2015, Gerrity et al. 2012), the semi-batch ozonation experiment has no dilution effect on the samples, which facilitates the measurement of BDOC. However, the determination of ozone dose becomes another important issue, as the rate of ozone mass transferred into water phase may change as a function of time. As shown in **Figure S1,** the transferred/absorbed ozone concentrations as a function of time were calculated based on measurements of the differential O_3 concentrations between the feed gas and off-gas streams, where the gaseous O_3 concentrations were measured by the modified indigo method (Chiou et al. 1995).

2.3. Batch biodegradation experiments

BDOC measurements were performed by quantifying the gross amount of DOC

degraded by an inoculum of suspended activated sludge over a predetermined period of time (Escobar and Randall 2001). In this study, a requisite amount of activated sludge from a WWTP was initially acclimated with glucose for 3 days. The acclimated activated sludge was washed by centrifugation and resuspended in deionized water 5 times prior to harvesting for BDOC measurements. Then 50 mL centrifuge tubes were filled with 40 ml water samples and spiked with 1 mL of the harvested activated sludge. The BDOC tests were conducted in duplicate and compared with results obtained using Milli-Q water as a blank control. A 200 mg/L dry biomass concentration was used in the tests. This dose was determined by weighing the biomass collected from ten test tubes after BDOC experiments; the biomass was dried at 105 ^{o}C before weighing. The inoculated centrifuge tubes were placed in an incubated shaker at 90 rpm and 25 ^{o}C for a period of 4 hours, following which the samples were centrifuged and the supernatants filtered through a 0.45μm PTFE filter for subsequent DOC and molecular weight analysis. The measured BDOC reflects the rapidly biodegradable fraction of BDOC that can be effectively removed by biofiltration; this fraction is thus referred to as $BDOC_{rapid}$ henceforth (Black and Berube 2014).

2.4. UV absorbance and fluorescence analysis

A HORIBA Aqualog spectrometer was used to simultaneously measure fluorescence EEM (Ex 220-450 nm / Em 245-825 nm) and UV absorbance spectra (220-450 nm). The samples' EEMs were automatically corrected for Raman scattering by subtracting the EEM of the water blank from the EEM of any surface water or wastewater sample. Inner filter effects were corrected using the instrument's software

that utilized applicable absorbance data.

The prototype LED UV/fluorescence sensor described in more detail in (Li et al. 2016a) uses a UV LED (280 ± 5 nm) as a light source and a photodiode to measure the intensity of light passing the cuvette. For fluorescence detection, the sensor uses blue light sensitive photodiodes combined with bandpass filters (330-355 nm and 415-490 nm) positioned at 90^{o} relative to the excitation beam to detect the protein-like and humic-like fluorescence, respectively. Inner filter effects in fluorescence signals detected by the sensor were corrected using the UVA280 values.

2.5. Molecular weight analysis

Analyses of DOC molecular weight distributions were performed by means of size exclusion chromatography with online carbon detection (SEC-OCD). These measurements utilized a DIONEX Ultimate3000 high-pressure liquid chromatography (HPLC) system coupled with an online organic carbon detector (Turbo Sievers 900 Portable TOC Analyzer, GE). A TOSOH Bioscience Toyopearl HW-50S size exclusion column was installed to separate DOM components with varying apparent MWs. The injection volume was 100 µL, and the column was eluted with 1 mL/min phosphate buffer (1.5 g/L Na_2HPO_4 * 2 H_2O + 2.5 g/L KH_2PO_4). Polyethylene glycol standards (PEG 20 kDa, 10 kDa, 6 kDa, 4 kDa, 1.5 kDa, 600 Da and 200 Da) from Alfa Aesar were used as apparent molecular weight (AMW) references. The SEC-OCD chromatograms for samples from each ozonation experiment were also processed with Shige software developed by Noda and Ozaki (2005) for 2D correlation analysis – the

goal of which was to ascertain potentially small variations of various spectra resulting from external perturbations, e.g., DOM ozonation in this study (supporting information **Figure S4**).

2.6. Bromide and bromate Analysis

Bromide concentrations were determined by means of IC-ICP-MS, using a PerkinElmer Series 200 HPLC coupled with a PerkinElmer SCIEX ELAN DRC-e ICP/MS Spectrometer. These analyses were done in accord with prior investigators (Shi and Adams 2009).

Bromate concentrations were determined by means of ion chromatography with MS/MS detection, using a Shimadzu Prominence LC-20 series HPLC system coupled with an API 4000 QTrap hybrid triple quadrupole/linear ion trap mass spectrometer (AB SCIEX) operating with negative mode electrospray ionization. Separations were performed using an ion exchange column (2 × 250 mm Dionex IonPac AS-16 w/ 2 × 50 mm AG-16 guard column**)** under isocratic conditions, with a mobile phase comprising 20% of a 1 mol/L aqueous methylamine solution and 80% of acetonitrile, at a flow rate of 0.25 mL/min and injection volume of 100 μL. The mass parameters used in multiple reaction monitoring mode for BrO_3^- identification and quantification were 128.9→113.0 and 126.9→110.8. Method detection and quantification limits for BrO_3^- were 0.03 and 0.1 μg/L, respectively.

3. Results and discussion

3.1. Degradation of chromophores

Absorbance spectra of water and wastewater ozonated at varying O_3/DOC ratios normalized by the original samples' absorbance spectra are shown in **Figure 1** and **Figure S2**. At all wavelengths > 230 nm, these spectra showed a monotonic decrease of absorbance associated with the increase of ozone dosage. Consistent with previous results (Chon et al. 2015, Gerrity et al. 2012), the normalized absorbance spectra were relatively flat in the wavelength range >250 nm. The flat region in the normalized absorbance spectra could be separated into sub-ranges below ~350 nm and above ~370 nm. At low ozone doses (O_3/DOC < 0.4), the observed variations of the normalized absorbance at λ < 350 nm were less pronounced than those of the relative residual absorbance at λ > 370 nm, and such relationships then reversed at the higher O_3/DOC ratios. This phenomenon indicates that the chromophores comprise at least two kinetically distinct functionalities during ozonation (Nanaboina and Korshin 2010). Due to its relatively high absolute value, the UV absorbance in the range of 250-300 nm presents a more convenient option for online monitoring than absorbance at λ > 300 nm.

Figure 2 illustrates that UVA254 and UVA280 represented as a function of O_3/DOC ratio or ozonation time exhibit similar changes. With the increase of O_3/DOC ratio, the UVA indices decreased steeply at low O_3/DOC ratios (< 0.5 mg O_3/mg DOC) and then decreased more gradually at higher O_3/DOC ratios. When presented vs. ozonation time, the normalized residual UVA indices decreased more steeply at the initial ozonation stage (< 40 s) and more gradually for longer ozonation times. This phenomenon could be explained by the contributions of kinetically different groups of

chromophores and also changes of the ozone transfer rate which varied as a function of time (**Figure S1**). The O_3/DOC ratios related to such inflection points were in the range of 0.4-0.6 mg O_3/mg DOC. At these O_3/DOC ratios, UVA254 and UVA280 were decreased by about 45-60 %. Given that the observed changes of the absorbance of ozonated water were similar for the two examined wavelengths, it can be concluded that measurements at 280 nm – a practically implementable LED emission wavelength feasible for online applications – may represent an excellent alternative to UVA254 measurements in the context of evaluation of ozonation efficiency as well as DBP formation during chlorination (Li et al. 2016a).

3.2. Degradation of fluorophores

Representative fluorescence excitation-emission matrixes (EEM) of untreated wastewater and surface water samples are shown in **Figure 3**. Generally, the fluorescence peaks with Em<380 nm are ascribed to protein-like fluorescence while the fluorescence peaks with Em>380 nm are ascribed to humic-like fluorescence associated with fluorophores comprising aromatic rings substituted with various electron-donating functional groups (Barsotti et al. 2016, Li et al. 2013, Li et al. 2015).

The examined wastewater samples showed the presence of two protein-like fluorescence peaks (Em ~ 350 nm) and two humic-like fluorescence peaks (Em ~ 430 nm), while the EEM of Lake Pleasant water was dominated by two humic-like fluorescence peaks (Em ~ 450 nm). The comparison of the fluorescence data obtained with the LED sensor and the lab benchtop spectrometer (**Table S1**) indicates a very

good convergence of these results and thus confirms the good sensitivity and accuracy of the LED sensor for use in online monitoring applications. However, the sensitivity of the LED sensor to humic-like fluorescence is much higher than to protein-like fluorescence, mainly due to the fluorescence integration area, the transmittance efficiency of the sensor's bandpass filter, and the response sensitivity of photodiodes to UV light. Due to the relatively weak contribution of protein-like fluorescence in Lake Pleasant samples, measurements of humic-like fluorescence are mainly discussed hereafter.

Figure 4 illustrates the degradation of humic-like fluorophores during ozonation. The humic-like fluorescence decreased very steeply at the initial stage of ozonation time (< 25 s) and then reached to a distinguishable flat region at high ozone time. Like for UVA254 and UVA280, the decrease of humic-like fluorescence as a function of O_3/DOC ratio could also be divided into two stages; however, more than 80% of the humic-like fluorescence was lost in the initial stage – much higher than for the UVA indices. The O_3/DOC ratios related to such inflection points between these two stages were in the range of 0.3-0.4.

3.3. Formation of BDOC

Figure 5a presents the formation of $BDOC_{rapid}$ as a function of O_3/DOC ratio or ozonation time. These data demonstrate that the formation of $BDOC_{rapid}$ increased gradually at O_3/DOC ratios < 0.4 and while it increased more steeply for O_3/DOC ratios 0.4-0.7. Above the latter transitional range of O_3/DOC ratios, $BDOC_{rapid}$ formation leveled off with distinguishable plateaus at higher O_3/DOC ratios, suggesting that the

289 remaining DOM is relatively refractory and requires more O_3 to be converted to the
290 biodegradable form. Similar patterns of BDOC formation at low O_3 doses were
291 observed in prior studies. For instance, Win et al. (2000) found that the biodegradability
292 of DOM was not appreciably affected by ozonation until a threshold of ozone dose was
293 reached. Liu et al. (2015) reported that there was no significant formation of aldehydes
294 and carboxylic acids that comprise a large part of the assimilable organic carbon (AOC)
295 in ozonated wastewater (DOC 7.8 mg/L) with O_3 dose less than 2 mg/L. The plateau in
296 $BDOC_{rapid}$ formation at higher O_3/DOC ratios is also consistent with prior observations
297 (Siddiqui et al. 1997, Treguer et al. 2010). When represented as a function of the
298 decrease of UV absorbance and fluorescence (**Figure 5b&c**), the $BDOC_{rapid}$
299 concentrations increased slowly in the initial stage and then rose more noticeably. The
300 inflection points in these plots corresponding to the decrease of UVA indices and
301 fluorescence were close to 35-45%, and 75-85%, respectively.

302 The degradation of DOM during ozonation can occur through either direct reaction
303 with O_3, or with $^{\bullet}OH$ radical generated during O_3 decomposition (von Gunten 2003a,
304 Wert et al. 2009). During the initial ozone demand stage (**Figure S3**), ozone reacts
305 directly and selectively with electron-rich moieties, e.g., aromatic chromophores or
306 fluorophores (Chon et al. 2015, Wert et al. 2009, Wu et al. 2016), resulting in the rapid
307 decreases of UV absorbance and fluorescence signals (**Figure 2** and **Figure 4**). Prior
308 research based on ozonation experiments (DOC 1.2-1.4 mg/L, O_3 2 mg/L) performed
309 with and without $^{\bullet}OH$ scavengers confirmed that direct ozone reactions are mainly
310 responsible for the formation of small organic compounds contributing to AOC during

311 the initial ozone demand stage (Hammes et al. 2006). However, such AOC molecules
312 might not be produced substantially at very low ozone dose (Liu et al. 2015). In the
313 present work, it is possible that the initial selective attacks of O_3 on electron-rich
314 moieties were not sufficient to break down the large MW DOM fractions into small
315 molecules associated with AOC, leading to the apparent lag in formation of $BDOC_{rapid}$
316 at O_3/DOC ratios < 0.4 The presence of small quantities of inorganic constituents that
317 might exert rapid O_3 demand at low O_3 doses (e.g., NO_2^-) also cannot be ruled out. With
318 greater O_3 doses, increasing exposure to O_3 and $^{\bullet}OH$ may have led to more extensive
319 breakdown of aromatic structures and other electron-rich targets through direct
320 reactions with O_3 and indirect reactions involving the much less selective $^{\bullet}OH$ (Legrini
321 et al. 1993, von Gunten 2003a). At O_3/DOC ratios above 0.4-0.7, the observed decrease
322 in formation of $BDOC_{rapid}$ may be attributable to accumulation of more O_3- and $^{\bullet}OH$-
323 recalcitrant products (e.g., acetic and oxalic acids) (Hammes et al. 2006, Ramseier and
324 Gunten 2009). The synergistic effect of O_3 and $^{\bullet}OH$ radical contributed to the sufficient
325 decomposition of large MW DOM and the prominent formation of AOCs.

326 **3.4. Evolution of DOM molecular weight during ozonation**

327 **Figure 6** shows the evolution of SEC-OCD chromatograms of WWTP effluent and
328 Lake Pleasant water during ozonation. In SEC experiments, DOM fractions with higher
329 apparent MW have lower elution times (**Figure S4**). Using peak assignments
330 introduced in prior research (Huber et al. 2011) to denote major features observed in
331 the data shown in **Figure 6**, both WWTP effluent and Lake Pleasant water had a
332 biopolymer-like peak of large AMW (peak a1 and peak b1, 20-30 min, AMW > 20

kDa). The WWTP effluent exhibited several peaks in the medium AMW range (peak a2, humic-like peak, 30-36 min, AMW of 14-5.5 kDa; peak a3, peak of building blocks, 36-40 min, AMW of 5.5-3 kDa) and two well-resolved peaks located at lower AMW values (peak a4, peak of low MW acids, 40-48 min, AMW of 3-0.8 kDa; peak a5, peak of low MW neutrals, 50-60 min, AMW < 800 Da). SEC-OCD data for Lake Pleasant water exhibited a prominent peak b2 (humic-like peak, 28-36 min, AMW of 20-5.5 kDa) with a shoulder b3 (building blocks, 36-40 min, AMW of 5.5-3 kDa). These peaks located in the range of medium AMW typically attributed to humic substances were responsible for a large portion of DOC in untreated Lake Pleasant water. The SEC-OCD of Lake Pleasant water also had two weaker peaks located in the range of small AMW (peak b4 and peak b5), which are designated as low MW acids and neutrals.

The evolution of apparent DOM molecular weights is indicated by the red arrows in **Figure 6.** It is also visualized using 2D synchronous correlation contours (**Figure S5**). At increasing ozone dosages, the large MW biopolymer-like peaks (a1 and b1) and medium MW humic-like peaks (a2 and b2) decreased while the concentration of building blocks and low MW acids and neutrals increased, suggesting that the larger AMW DOM components were transformed into smaller AMW species during ozonation. The newly formed medium building blocks and small MW DOM species were easily biodegraded and mainly contributed to the $BDOC_{rapid}$ (**Figure S6**). The SEC-OCD results also confirmed that the decomposition of biopolymer-like or humic-like peaks was not prominent (<20%) during the initial ozonation stage, despite the substantial losses of UVA and fluorescence (**Figure S7**).

3.5. Formation of bromate

Figures 7a-b depict bromate yields (expressed as mol ratios of Br associated with BrO_3^- to initial Br^- ($[BrO_3^-]/[Br^-]$, in % mol/mol) plotted as a function of O_3/DOC ratio or ozonation time. The observed relationships exhibit the presence of two phases of bromate formation, as marked by the dash line. During the initial phase (O_3/DOC ratios < 0.4 or ozonation time < 25 s), bromate yields were low ($[BrO_3^-]/[Br^-]$ < 2 %) and effects of initial Br^- concentrations on this phase were minor. This is in agreement with the data of previous studies (Chon et al. 2015, Soltermann et al. 2016), which observed a negligible bromate yield (≤3%) for O_3/DOC ratios < 0.4-0.6 mg O_3/mg DOC.

This phenomenon can be ascribed to specific features of the formation pathway of bromate, which is generated via a complex mechanism involving ozone and hydroxyl radical (Fischbacher et al. 2015, von Gunten and Oliveras 1998). During the initial phase of bromate formation (O_3/DOC ratios < 0.4, ozonation time < 25 s), O_3 is rapidly consumed by electron-rich moieties (Buffle et al. 2006, Lee et al. 2013) whose consumption is consistent with the rapid decrease of humic-like fluorescence (**Figure 4),** thus leaving little residual O_3 for reaction with Br^- (**Figure S3**). In the second phase, in which measured residual ozone concentrations exceeded 1 mg/L (**Figure S3**), bromide could be readily oxidized to bromate, with its yields increasing with the ozone doses, and different water matrixes had a significant effect on the bromate yields measured as a function of O_3/DOC ratio or ozonation time.

When plotted versus O_3/DOC ratio, the bromate formation across different water

matrixes was similar for each matrix when presented in terms of bromate concentration in μg/L (**Figure S8**), but different when represented in terms of bromate yield units (**Figure 7**). That is, the lower initial bromide concentration in Lake Pleasant water led to higher molar bromate yields compared to those for the higher-bromide WWTP effluent samples at the same ozone doses. Compared with the data of the previous study (Chon et al. 2015), the bromate formation yields of WWTP effluent samples at the corresponding O_3/DOC ratios in the present work were lower, possibly due to the higher initial Br^- concentrations in this study (Br^- 300-500 μg/L for DOC 5.8-6.9 mg/L vs. Br^- 39-86 μg/L for DOC 5.3-7.3 mg/L). Therefore, the O_3/DOC ratio might not always be an optimal indicator for estimation of bromate formation across different water matrixes.

Figures 7c-d present the normalized bromate yields ($[BrO_3^-]/[Br^-]$, mol/mol) as a function of relative changes in the spectroscopic parameters UVA254, UVA280 and humic-like fluorescence. In agreement with one previous study (Chon et al. 2015), the plots of bromate yields vs. spectroscopic indicators overlapped for all data sets obtained in the ozonation experiments, although the DOM properties and initial Br^- concentrations were different. Similarly to the observations discussed above, changes in the bromate yields could be further divided into two stages characterized by significantly different slopes vs. corresponding spectroscopic index. The inflection points related to the appreciable formation of BrO_3^- were in the range of 45-55%, 50-60% and 86-92% losses of UVA254, UVA280, and humic-like fluorescence, respectively. Unlike O_3/DOC ratios, the plots of $[BrO_3^-]/[Br^-]$ as a function of the spectroscopic indicators in the second phase had relatively small differences for the

398 data obtained for Lake Pleasant and WWTP effluent samples, suggesting that the
399 spectroscopic indices may be more suitable as a surrogate parameter for bromate
400 formation in waters of varying composition.

401 With respect to the US EPA's MCL for BrO_3^- in drinking water of 10 μg/L, the
402 breakthrough points related to removals of UVA254, UVA280 and decrease of humic-
403 like fluorescence were in the range of 45-55%, 52-57%, and 86-90%, respectively
404 (**Figure 8**). In contrast to the observations made for $[BrO_3^-]/[Br^-]$ molar yields (**Figure**
405 **7**), plots of BrO_3^- vs UVA254 and BrO_3^- vs UVA280 diverged into distinct groups of
406 data for WWTP effluents and Lake Pleasant. Such divergences were presumably due
407 to differences in initial Br^- concentrations in the various matrixes, since BrO_3^- yields
408 were not normalized to initial Br^- levels in these plots. Additionally, chromophores in
409 Lake Pleasant water appeared to be much more susceptible to the oxidation at higher
410 O_3 exposures than chromophores in WWTP effluents (**Figure 2**). However, no
411 significant divergences between the data for dissimilar water matrixes were observed
412 in plots of BrO_3^- vs humic fluorescence. In comparison to the ~25% variation amongst
413 UVA indices in the various matrixes at higher O_3 exposures, further decreases of
414 humic-like fluorescence were limited in a narrow range from 90% to 100%. The
415 association of this narrow range of changes of humic-like fluorescence with the
416 generation of bromate is likely to have largely eliminated any divergence attributable
417 to differences in initial Br^- concentration. A previous study also reported a sole
418 correlation between a fluorescence index and several chlorinated DBPs regardless of
419 the water source and treatment, while the differential absorbance correlations could be

interfered by many species (Roccaro et al. 2009). These results showed that fluorescence indices may have more advantages than absorbance indices in actual water systems.

The plots of BrO_3^- concentration (μg/L) versus decrease of humic fluorescence (HS, in %) were fitted by MATLAB software (**Figure S9**), and an empirical equation applicable to the ranges of 6-7 mg/L DOC and 100-500 μg/L Br^- was obtained, as presented below:

$$BrO_3^- \ (\mu g/L) = 7.64 * 10^{-9} * e^{0.237*HS(\%)}, R^2 = 0.962$$

The results of this study suggest that measurements of changes in humic-like fluorescence of ozonated water are highly suitable for the estimation of bromate formation in dissimilar water matrixes. The results in **Figure S10** further indicate that DOC concentration has relatively little effect on the relationships between bromate formation and humic-like fluorescence. However, the robustness of such relationships still needs to be explored in the future; for example, with respect to the effects of pH, temperature, DOC and NH_4^+ concentrations.

In the context of optimization of ozone dosage, the typical goal is to maximize the effect of oxidation while simultaneously minimizing the formation of undesired byproducts. Gerrity et al. (2012) previously reported that ~50% reduction of UVA254 or ~90% decrease of total fluorescence were required to reach acceptable levels of pathogen inactivation and sufficient elimination of many micropollutants. The present work supports these findings and demonstrates possible approaches for assessing the

potential formation of BDOC and bromate during water and wastewater ozonation, especially for water having bromide concentrations above 50 μg/L.

4. Conclusions

- When represented as a function of changes of spectroscopic indicators such as UVA254, UVA280, and humic-like fluorescence, BDOC concentrations initially increased slowly and then rose more noticeably. The inflection points indicative of BDOC formation threshold were located in the range of 35-45% loss of UVA254 or UVA280 and 75-85% loss of humic-like fluorescence.

- SEC-OCD data showed that large biopolymer molecules in WWTP effluent (apparent MW>20 kDa) and medium-AMW humic substances in Lake Pleasant surface water (AMW 5.5-20 kDa) were transformed into medium-AMW building blocks and small AMW species associated with BDOC.

- When represented as a function of spectroscopic indicators, the inflection points that corresponded to the onset of bromate formation were approximately 45-55%, 50-60% and 86-92% for decreases in UVA254, UVA280 and humic fluorescence, respectively.

- An empirical equation modeling the relationship between bromate concentrations (expressed in μg/L) and concomitant decreases of humic-like fluorescence (%) was established based on the data generated for wastewater effluent and surface water that had 100 to 500 μg/L Br^-.

- The results suggest that measurements of UVA280 and humic-like fluorescence

complement conventional UVA254 measurements, especially in the context of assessing the formation of BDOC and bromate. The use of these spectroscopic parameters is expected to be enhanced by the recent development of online/portable spectrometers that use LEDs as a light source.

Acknowledgement

We thank the generous support from National Key R&D Program (No. 2016YFE0112300), National Science Foundation of China (No. 51438008) and MADFORWATER (No. 688320) for the development of LED UV fluorescence sensor. We also acknowledge the support for Tessora Young from her NSF graduate research fellowship. Wentao Li thanks the scholarship from the China Scholarship Council (No. 201506190059) and Shanghai Tongji GaoTingyao Environmental Science & Technology Development Foundation (STGEF).

Appendix A. Supplementary data

Supplementary data related to this article can be found in Supporting Information.

References

Bader, H. and Hoigné, J., 1981. Determination of ozone in water by the indigo method. Water Research 15 (4), 449-456.

Barsotti, F., Ghigo, G. and Vione, D., 2016. Computational assessment of the fluorescence emission of phenol oligomers: A possible insight into the fluorescence properties of humic-like substances (HULIS). Journal of Photochemistry and Photobiology a-Chemistry 315, 87-93.

Black, K.E. and Berube, P.R., 2014. Rate and extent NOM removal during oxidation and biofiltration. Water Research 52, 40-50.

Bridgeman, J., Baker, A., Brown, D. and Boxall, J.B., 2015. Portable LED fluorescence instrumentation for the rapid assessment of potable water quality. Science of The Total Environment 524–525, 338-346.

Buffle, M.-O., Schumacher, J., Salhi, E., Jekel, M. and von Gunten, U., 2006. Measurement of the initial phase of ozone decomposition in water and wastewater by means of a continuous quench-flow system: Application to disinfection and pharmaceutical oxidation. Water Research 40 (9), 1884-1894.

Butler, R., Godley, A., Lytton, L. and Cartmell, E., 2005. Bromate environmental contamination: Review of impact and possible treatment. Critical Reviews in Environmental Science and Technology 35 (3), 193-217.

Chin, Y.-P., Aiken, G. and O'Loughlin, E., 1994. Molecular Weight, Polydispersity, and Spectroscopic Properties of Aquatic Humic Substances. Environmental Science & Technology 28 (11), 1853-1858.

Chiou, C.F., Marinas, B.J. and Adams, J.Q., 1995. Modified indigo method for gaseous and aqueous ozone analyses. Ozone-Science & Engineering 17 (3), 329-344.

Chon, K., Salhi, E. and von Gunten, U., 2015. Combination of UV absorbance and electron donating capacity to assess degradation of micropollutants and formation of bromate during ozonation of wastewater effluents. Water Research 81, 388-397.

Dodd, M.C., Kohler, H.P.E. and von Gunten, U., 2009. Oxidation of Antibacterial Compounds by Ozone and Hydroxyl Radical: Elimination of Biological Activity during Aqueous Ozonation Processes. Environmental Science & Technology 43 (7), 2498-2504.

Escobar, I.C. and Randall, A.A., 2001. Assimilable organic carbon (AOC) and biodegradable dissolved organic carbon (BDOC): Complementary measurements. Water Research 35 (18), 4444-4454.

Fimmen, R.L., Cory, R.M., Chin, Y.-P., Trouts, T.D. and McKnight, D.M., 2007. Probing the oxidation–reduction properties of terrestrially and microbially derived dissolved organic matter. Geochimica et Cosmochimica Acta 71 (12), 3003-3015.

Fischbacher, A., Loeppenberg, K., von Sonntag, C. and Schmidt, T.C., 2015. A New Reaction Pathway for Bromite to Bromate in the Ozonation of Bromide. Environmental Science & Technology 49 (19), 11714-11720.

Gerrity, D., Gamage, S., Jones, D., Korshin, G.V., Lee, Y., Pisarenko, A., Trenholm, R.A., von Gunten, U., Wert, E.C. and Snyder, S.A., 2012. Development of surrogate correlation models to predict trace organic contaminant oxidation and microbial inactivation during ozonation. Water Research 46 (19), 6257-6272.

520 Hammes, F., Salhi, E., Koster, O., Kaiser, H.P., Egli, T. and von Gunten, U., 2006.
521 Mechanistic and kinetic evaluation of organic disinfection by-product and
522 assimilable organic carbon (AOC) formation during the ozonation of drinking
523 water. Water Research 40 (12), 2275-2286.
524 Henderson, R.K., Baker, A., Murphy, K.R., Hambly, A., Stuetz, R.M. and Khan, S.J.,
525 2009. Fluorescence as a potential monitoring tool for recycled water systems: A
526 review. Water Research 43 (4), 863-881.
527 Hollender, J., Zimmermann, S.G., Koepke, S., Krauss, M., McArdell, C.S., Ort, C.,
528 Singer, H., von Gunten, U. and Siegrist, H., 2009. Elimination of Organic
529 Micropollutants in a Municipal Wastewater Treatment Plant Upgraded with a Full-
530 Scale Post-Ozonation Followed by Sand Filtration. Environmental Science &
531 Technology 43 (20), 7862-7869.
532 Huber, M.M., Gobel, A., Joss, A., Hermann, N., Loffler, D., McArdell, C.S., Ried, A.,
533 Siegrist, H., Ternes, T.A. and von Gunten, U., 2005. Oxidation of pharmaceuticals
534 during ozonation of municipal wastewater effluents: A pilot study. Environmental
535 Science & Technology 39 (11), 4290-4299.
536 Huber, S.A., Balz, A., Abert, M. and Pronk, W., 2011. Characterisation of aquatic
537 humic and non-humic matter with size-exclusion chromatography – organic
538 carbon detection – organic nitrogen detection (LC-OCD-OND). Water Research
539 45 (2), 879-885.
540 Lee, C.O., Howe, K.J. and Thomson, B.M., 2012. Ozone and biofiltration as an
541 alternative to reverse osmosis for removing PPCPs and micropollutants from

542 treated wastewater. Water Research 46 (4), 1005-1014.
543 Lee, Y., Gerrity, D., Lee, M., Bogeat, A.E., Salhi, E., Gamage, S., Trenholm, R.A.,
544 Wert, E.C., Snyder, S.A. and von Gunten, U., 2013. Prediction of Micropollutant
545 Elimination during Ozonation of Municipal Wastewater Effluents: Use of Kinetic
546 and Water Specific Information. Environmental Science & Technology 47 (11),
547 5872-5881.
548 Legrini, O., Oliveros, E. and Braun, A.M., 1993. Photochemical processes for water
549 treatment. Chemical Reviews 93 (2), 671-698.
550 Li, W.-T., Jin, J., Li, Q., Wu, C.-F., Lu, H., Zhou, Q. and Li, A.-M., 2016a. Developing
551 LED UV fluorescence sensors for online monitoring DOM and predicting DBPs
552 formation potential during water treatment. Water Research 93, 1-9.
553 Li, W.-T., Xu, Z.-X., Li, A.-M., Wu, W., Zhou, Q. and Wang, J.-N., 2013.
554 HPLC/HPSEC-FLD with multi-excitation/emission scan for EEM interpretation
555 and dissolved organic matter analysis. Water Research 47 (3), 1246-1256.
556 Li, W., Nanaboina, V., Chen, F. and Korshin, G.V., 2016b. Removal of polycyclic
557 synthetic musks and antineoplastic drugs in ozonated wastewater: Quantitation
558 based on the data of differential spectroscopy. Journal of Hazardous Materials 304,
559 242-250.
560 Li, W., Xu, Z., Wu, Q., Li, Y., Shuang, C. and Li, A., 2015. Characterization of
561 fluorescent-dissolved organic matter and identification of specific fluorophores in
562 textile effluents. Environmental Science and Pollution Research 22 (6), 4183-4189.
563 Liu, C., Nanaboina, V. and Korshin, G., 2012a. Spectroscopic study of the degradation

564 of antibiotics and the generation of representative EfOM oxidation products in
565 ozonated wastewater. Chemosphere 86 (8), 774-782.
566 Liu, C., Nanaboina, V., Korshin, G.V. and Jiang, W., 2012b. Spectroscopic study of
567 degradation products of ciprofloxacin, norfloxacin and lomefloxacin formed in
568 ozonated wastewater. Water Research 46 (16), 5235-5246.
569 Liu, C., Tang, X., Kim, J. and Korshin, G.V., 2015. Formation of aldehydes and
570 carboxylic acids in ozonated surface water and wastewater: A clear relationship
571 with fluorescence changes. Chemosphere 125, 182-190.
572 Nakada, N., Shinohara, H., Murata, A., Kiri, K., Managaki, S., Sato, N. and Takada, H.,
573 2007. Removal of selected pharmaceuticals and personal care products (PPCPs)
574 and endocrine-disrupting chemicals (EDCs) during sand filtration and ozonation
575 at a municipal sewage treatment plant. Water Research 41 (19), 4373-4382.
576 Nanaboina, V. and Korshin, G.V., 2010. Evolution of Absorbance Spectra of Ozonated
577 Wastewater and Its Relationship with the Degradation of Trace-Level Organic
578 Species. Environmental Science & Technology 44 (16), 6130-6137.
579 Nie, Y., Hu, C., Li, N., Yang, L. and Qu, J., 2014. Inhibition of bromate formation by
580 surface reduction in catalytic ozonation of organic pollutants over beta-
581 FeOOH/Al2O3. Applied Catalysis B-Environmental 147, 287-292.
582 Nishijima, W., Fahmi, Mukaidani, T. and Okada, M., 2003. DOC removal by multi-
583 stage ozonation-biological treatment. Water Research 37 (1), 150-154.
584 Noda, I. and Ozaki, Y. (2005) Two-dimensional correlation spectroscopy: applications
585 in vibrational and optical spectroscopy, John Wiley & Sons.

586 Peter, A. and von Gunten, U., 2007. Oxidation kinetics of selected taste and odor
587 compounds during ozonation of drinking water. Environmental Science &
588 Technology 41 (2), 626-631.
589 Ramseier, M.K. and Gunten, U.v., 2009. Mechanisms of Phenol Ozonation—Kinetics
590 of Formation of Primary and Secondary Reaction Products. Ozone: Science &
591 Engineering 31 (3), 201-215.
592 Reungoat, J., Escher, B.I., Macova, M., Argaud, F.X., Gernjak, W. and Keller, J., 2012.
593 Ozonation and biological activated carbon filtration of wastewater treatment plant
594 effluents. Water Research 46 (3), 863-872.
595 Roccaro, P., Vagliasindi, F.G.A. and Korshin, G.V., 2009. Changes in NOM
596 Fluorescence Caused by Chlorination and their Associations with Disinfection by-
597 Products Formation. Environmental Science & Technology 43 (3), 724-729.
598 Shi, H. and Adams, C., 2009. Rapid IC–ICP/MS method for simultaneous analysis of
599 iodoacetic acids, bromoacetic acids, bromate, and other related halogenated
600 compounds in water. Talanta 79 (2), 523-527.
601 Siddiqui, M.S., Amy, G.L. and Murphy, B.D., 1997. Ozone enhanced removal of
602 natural organic matter from drinking water sources. Water Research 31 (12), 3098-
603 3106.
604 Soltermann, F., Abegglen, C., Götz, C. and von Gunten, U., 2016. Bromide Sources
605 and Loads in Swiss Surface Waters and Their Relevance for Bromate Formation
606 during Wastewater Ozonation. Environmental Science & Technology 50 (18),
607 9825-9834.

608 Tedetti, M., Joffre, P. and Goutx, M., 2013. Development of a field-portable
609 fluorometer based on deep ultraviolet LEDs for the detection of phenanthrene- and
610 tryptophan-like compounds in natural waters. Sensors and Actuators B-Chemical
611 182, 416-423.
612 Treguer, R., Tatin, R., Couvert, A., Wolbert, D. and Tazi-Pain, A., 2010. Ozonation
613 effect on natural organic matter adsorption and biodegradation - Application to a
614 membrane bioreactor containing activated carbon for drinking water production.
615 Water Research 44 (3), 781-788.
616 von Gunten, U., 2003a. Ozonation of drinking water: Part I. Oxidation kinetics and
617 product formation. Water Research 37 (7), 1443-1467.
618 von Gunten, U., 2003b. Ozonation of drinking water: Part II. Disinfection and by-
619 product formation in presence of bromide, iodide or chlorine. Water Research 37
620 (7), 1469-1487.
621 von Gunten, U. and Oliveras, Y., 1998. Advanced Oxidation of Bromide-Containing
622 Waters: Bromate Formation Mechanisms. Environmental Science & Technology
623 32 (1), 63-70.
624 Wert, E.C., Rosario-Ortiz, F.L., Drury, D.D. and Snyder, S.A., 2007. Formation of
625 oxidation byproducts from ozonation of wastewater. Water Research 41 (7), 1481-
626 1490.
627 Wert, E.C., Rosario-Ortiz, F.L. and Snyder, S.A., 2009. Using Ultraviolet Absorbance
628 and Color To Assess Pharmaceutical Oxidation during Ozonation of Wastewater.
629 Environmental Science & Technology 43 (13), 4858-4863.

630 Wu, Q., Li, W.T., Yu, W.H., Li, Y. and Li, A.M., 2016. Removal of fluorescent
631 dissolved organic matter in biologically treated textile wastewater by ozonation-
632 biological aerated filter. Journal of the Taiwan Institute of Chemical Engineers 59,
633 359-364.
634 Zimmermann, S.G., Wittenwiler, M., Hollender, J., Krauss, M., Ort, C., Siegrist, H. and
635 von Gunten, U., 2011. Kinetic assessment and modeling of an ozonation step for
636 full-scale municipal wastewater treatment: Micropollutant oxidation, by-product
637 formation and disinfection. Water Research 45 (2), 605-617.
638

639 **Table 1. Basic characteristics of water matrixes**

Parameters	WWTP-I	WWTP-II	Lake Pleasant
pH	6.92	6.95	7.48 [a]
DOC (mg/L)	5.82	6.93	14.87
UV254 (cm^{-1})	0.130	0.139	0.727
UV280 (cm^{-1})	0.100	0.108	0.545
Conductivity (us/cm)	480	652	314
Br^- (µg/L) [b]	267.8	201.5	36.7

[a] The pH values of 2.5 times diluted lake Pleasant water were about 7.

[b] The values listed here are the native background Br^- concentrations for each water matrix. Initial Br^- concentrations during ozonation batch experiments, using samples of each water matrix fortified with additional bromide, were as follows: 322.9 µg/L for WWTP-A, 373.8 µg/L for WWTP-B, 491.6 µg/L for WWTP-C, 301.5 µg/L for WWTP-D, and 116.1 µg/L for LP.

640

Figure Captions

Figure 1. Changes in the absorbance spectra of WWTP effluent as a function of O_3/DOC ratio normalized by the absorbance prior to treatment

Figure 2. Decreases of the normalized residual UVA indices as a function of O_3/DOC ratio (or ozonation time – inserts): (a) UVA254 and (b) UVA280

Figure 3. EEM spectra of (a) WWTP-I, (b) WWTP-II, and (c) LP. The circles on the left of each graph represent protein-like fluorescence that the LED sensor measures, while the circles on the right of each graph represent humic-like fluorescence that the LED sensor measures.

Figure 4. Decrease of the normalized humic-like fluorescence (H/H_0) as a function of O_3/DOC ratio or ozonation time (insert) in different ozonation experiments

Figure 5. Formation of $BDOC_{rapid}$ as a function of (a) O_3/DOC ratio or ozonation time (insert), (b) decrease of UVA254 or UVA280 (insert) and (c) decrease of LED humic-like fluorescence

Figure 6. Evolution of SEC-OCD chromatograms of the ozonated wastewater and surface water as a function of O_3/DOC ratio：(a) WWTP-I effluent (WWTP-A) and (b) Lake Pleasant water (LP).

Figure 7. Bromate formation yields ($[BrO_3^-]/[Br^-]$, mol/mol in %) represented as a function of (a) O_3/DOC ratio, (b) ozonation time, (c) decrease of UVA254 or UVA280 (insert) and (d) decrease of LED humic-like fluorescence.

Figure 8. Bromate formation (μg/L) as a function of decreases of spectral indicators: (a) UVA254 or UVA280 (insert) and (b) LED humic-like fluorescence

Figure 1

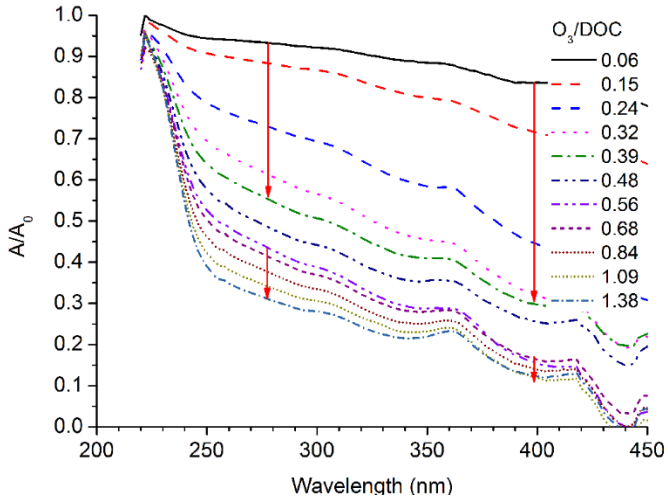

Figure 2

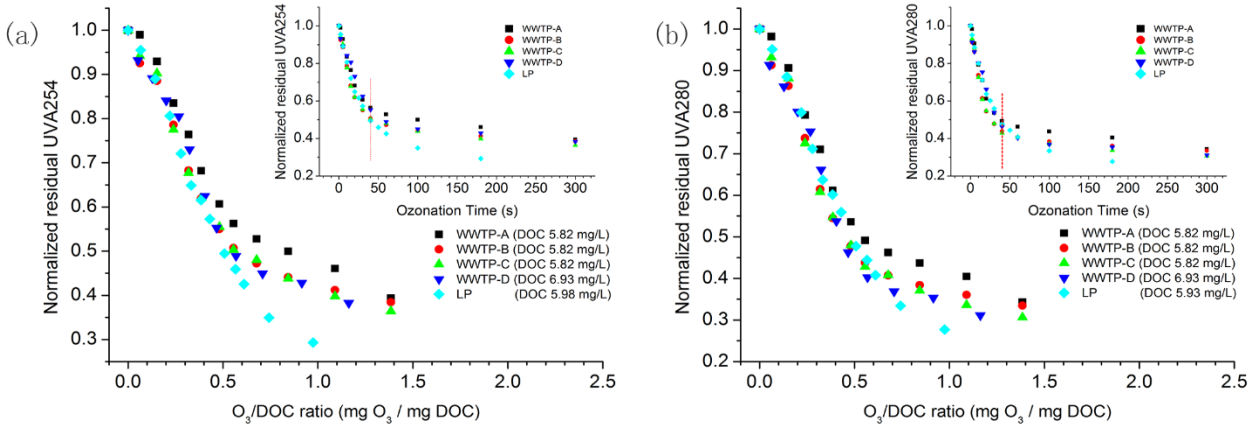

Figure 3

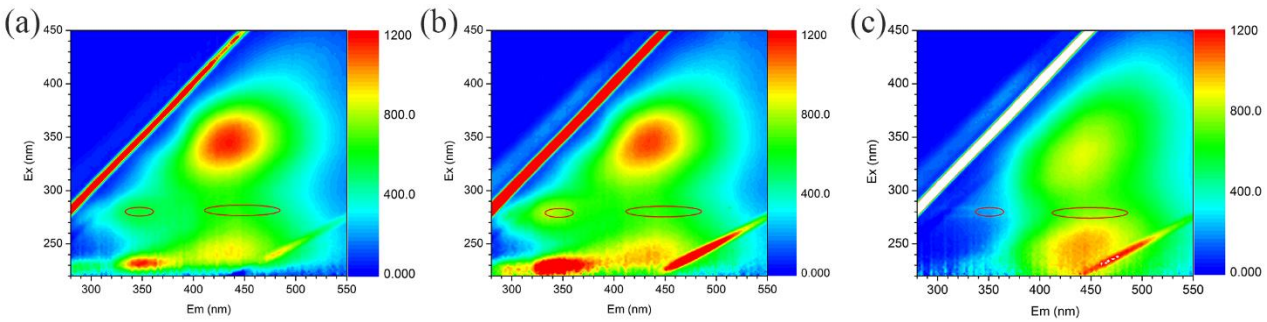

Figure 4

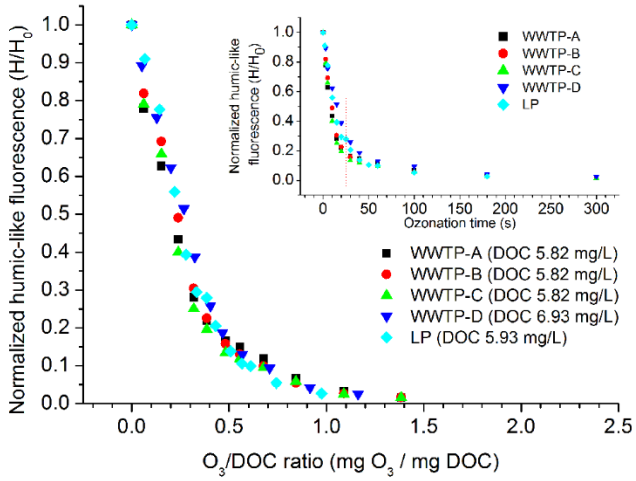
Normalized humic-like fluorescence (H/H0)
O3/DOC ratio (mg O3 / mg DOC)
Normalized humic-like fluorescence (H/H0)
Ozonation time (s)
WWTP-A
WWTP-B
WWTP-C
WWTP-D
LP
WWTP-A (DOC 5.82 mg/L)
WWTP-B (DOC 5.82 mg/L)
WWTP-C (DOC 5.82 mg/L)
WWTP-D (DOC 6.93 mg/L)
LP (DOC 5.93 mg/L)

Figure 5

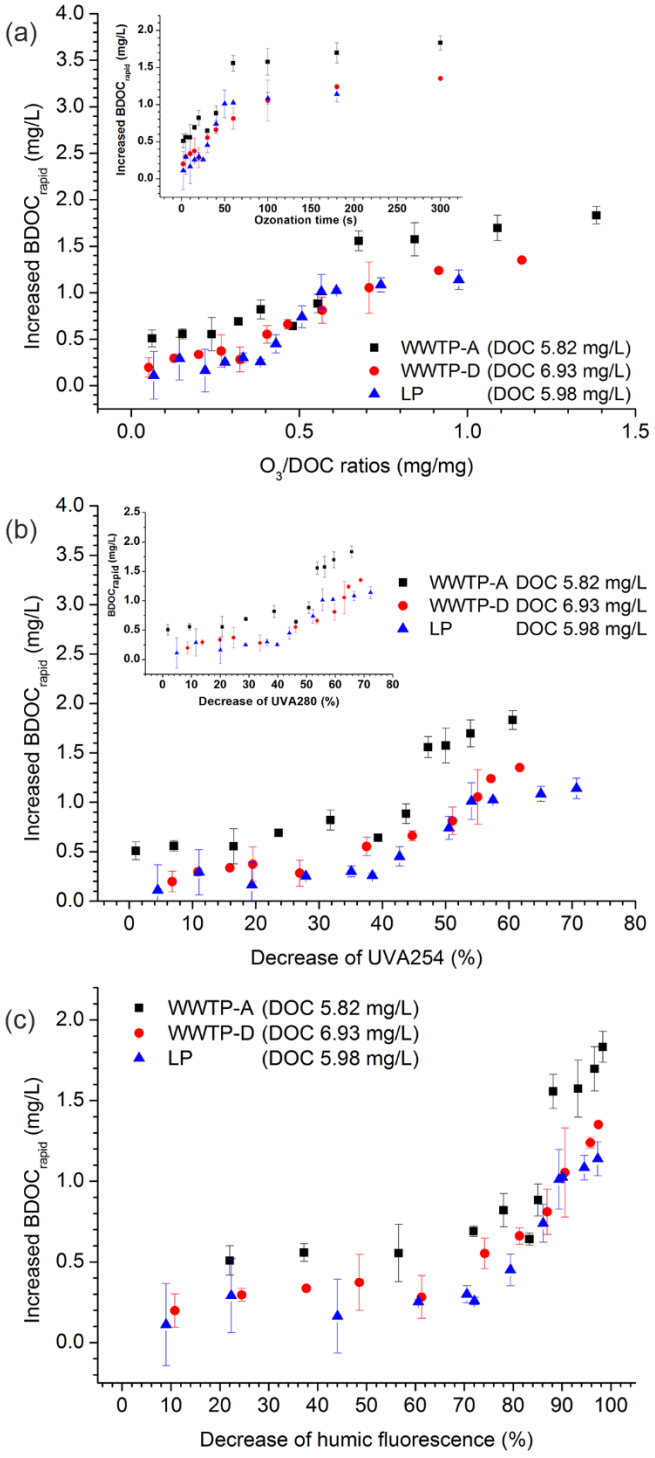
(a)
Increased BDOC$_{rapid}$ (mg/L)
Increased BDOC$_{rapid}$ (mg/L)
Ozonation time (s)
WWTP-A (DOC 5.82 mg/L)
WWTP-D (DOC 6.93 mg/L)
LP (DOC 5.98 mg/L)
O$_3$/DOC ratios (mg/mg)
(b)
Increased BDOC$_{rapid}$ (mg/L)
BDOC$_{rapid}$ (mg/L)
Decrease of UVA280 (%)
WWTP-A DOC 5.82 mg/L
WWTP-D DOC 6.93 mg/L
LP DOC 5.98 mg/L
Decrease of UVA254 (%)
(c)
Increased BDOC$_{rapid}$ (mg/L)
WWTP-A (DOC 5.82 mg/L)
WWTP-D (DOC 6.93 mg/L)
LP (DOC 5.98 mg/L)
Decrease of humic fluorescence (%)

Figure 6

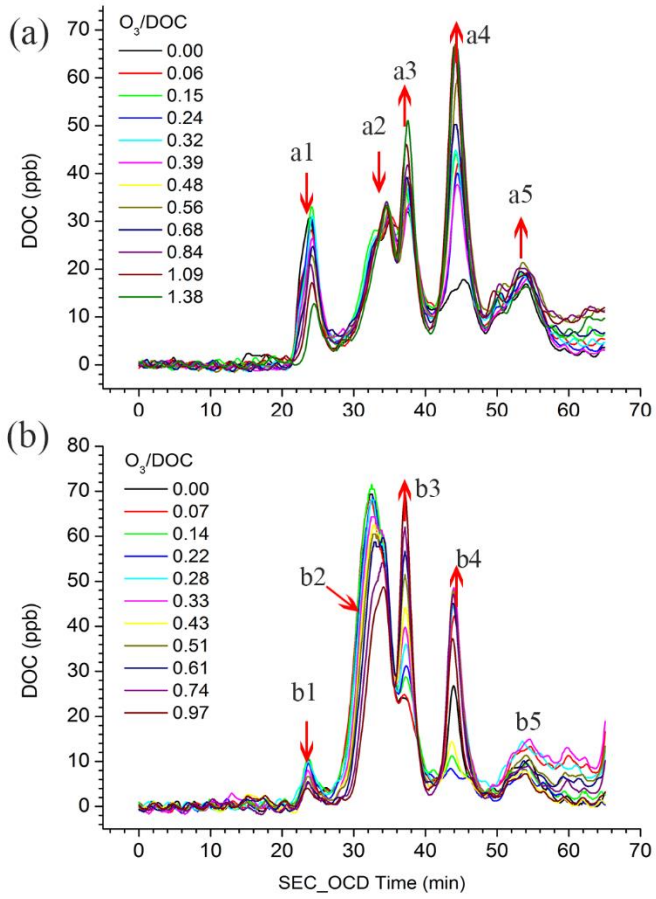
(a)
O3/DOC
0.00
0.06
0.15
0.24
0.32
0.39
0.48
0.56
0.68
0.84
1.09
1.38
a1
a2
a3
a4
a5
DOC (ppb)
(b)
O3/DOC
0.00
0.07
0.14
0.22
0.28
0.33
0.43
0.51
0.61
0.74
0.97
b1
b2
b3
b4
b5
DOC (ppb)
SEC_OCD Time (min)

Figure 7

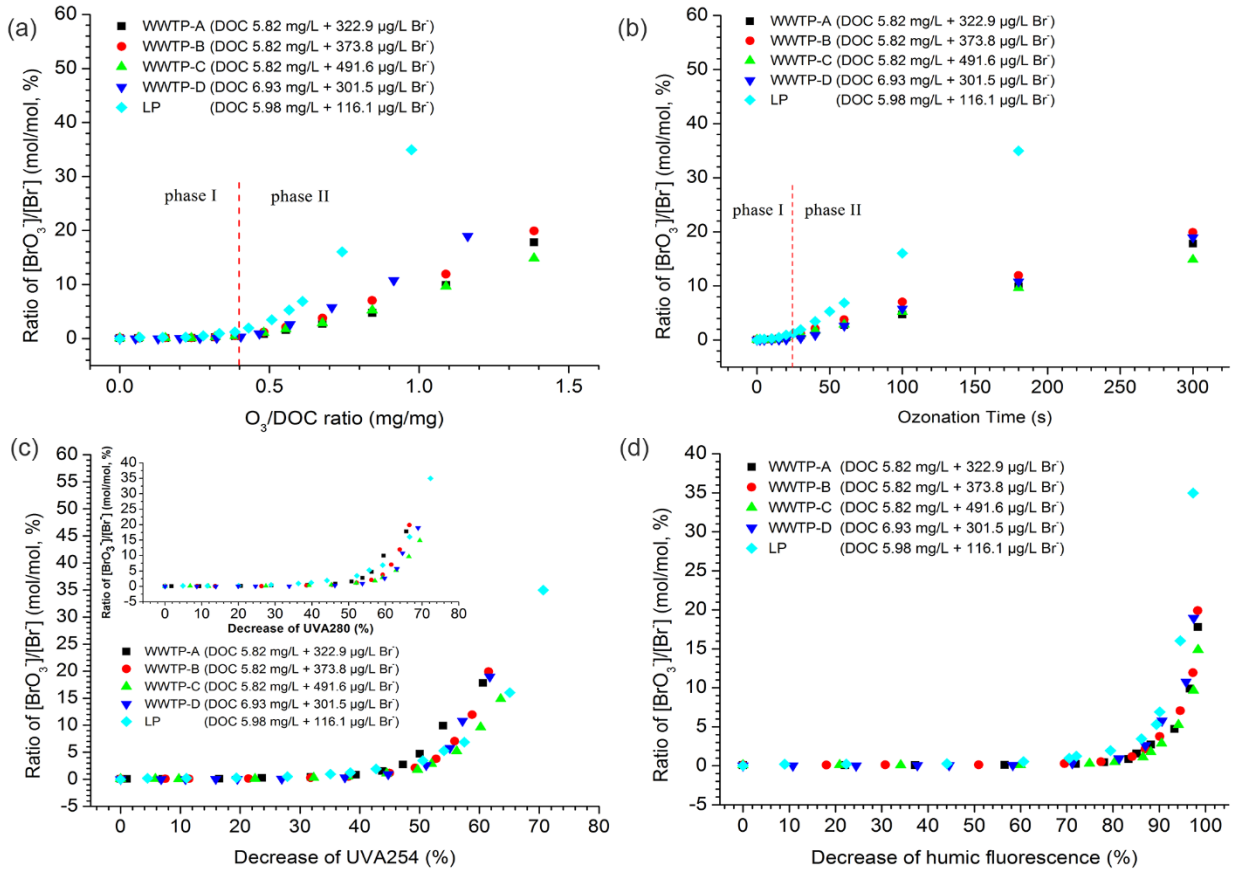
(a)
WWTP-A (DOC 5.82 mg/L + 322.9 μg/L Br⁻)
WWTP-B (DOC 5.82 mg/L + 373.8 μg/L Br⁻)
WWTP-C (DOC 5.82 mg/L + 491.6 μg/L Br⁻)
WWTP-D (DOC 6.93 mg/L + 301.5 μg/L Br⁻)
LP (DOC 5.98 mg/L + 116.1 μg/L Br⁻)
phase I
phase II
Ratio of [BrO3⁻]/[Br⁻] (mol/mol, %)
O3/DOC ratio (mg/mg)
(b)
Ozonation Time (s)
(c)
Decrease of UVA280 (%)
Decrease of UVA254 (%)
(d)
Decrease of humic fluorescence (%)

Figure 8

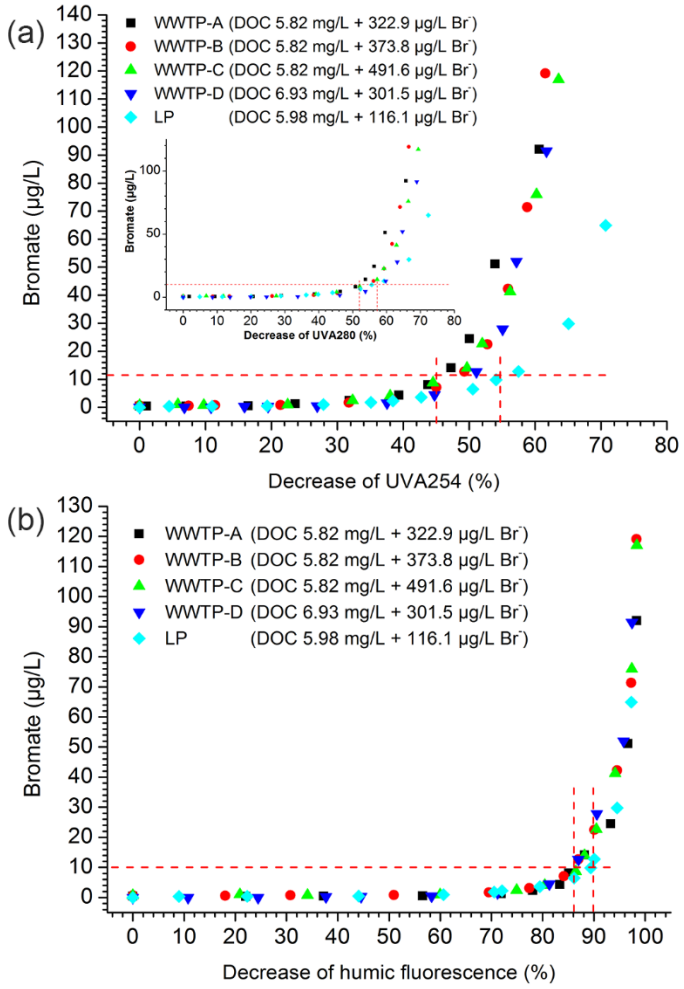
(a)
WWTP-A (DOC 5.82 mg/L + 322.9 μg/L Br-)
WWTP-B (DOC 5.82 mg/L + 373.8 μg/L Br-)
WWTP-C (DOC 5.82 mg/L + 491.6 μg/L Br-)
WWTP-D (DOC 6.93 mg/L + 301.5 μg/L Br-)
LP (DOC 5.98 mg/L + 116.1 μg/L Br-)
Bromate (μg/L)
Decrease of UVA254 (%)
Bromate (μg/L)
Decrease of UVA280 (%)
(b)
WWTP-A (DOC 5.82 mg/L + 322.9 μg/L Br-)
WWTP-B (DOC 5.82 mg/L + 373.8 μg/L Br-)
WWTP-C (DOC 5.82 mg/L + 491.6 μg/L Br-)
WWTP-D (DOC 6.93 mg/L + 301.5 μg/L Br-)
LP (DOC 5.98 mg/L + 116.1 μg/L Br-)
Bromate (μg/L)
Decrease of humic fluorescence (%)